

Supplementary Information

Polydopamine-coated cerium oxide core-shell nanoparticles for efficient and non-damaging chemical-mechanical polishing

Xiaohai He,^a Bo Gao,^a Qingyuan Wu,^b Chengrui Xin,^a Junjie Xue,^a

Fangwei Lu,^a Xin-Ping Qu,^c Simin Li,^{*a} Fan Zhang,^{*a} Hui Shen^{*a}

^aThe College of Energy Materials and Chemistry, Inner Mongolia University, Hohhot 010021, China.

^bNew Cornerstone Science Laboratory, State Key Laboratory for Physical Chemistry of Solid Surfaces, Collaborative Innovation Center of Chemistry for Energy Materials, and National & Local Joint Engineering Research Center of Preparation Technology of Nanomaterials, College of Chemistry and Chemical Engineering, Xiamen University, Xiamen 361005, China.

^cSchool of Microelectronics, Fudan University, Shanghai, 200433, China.

Email: shen@imu.edu.cn (H.S.); siminli@imu.edu.cn (S.L.)

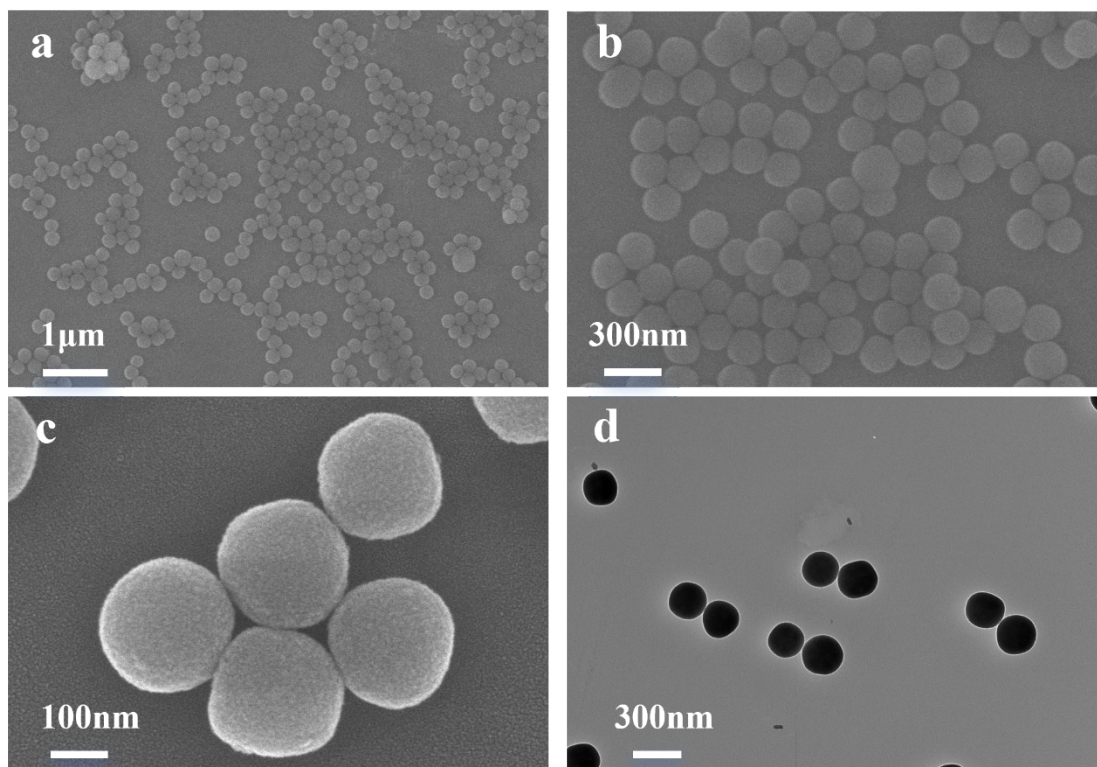


Figure S1. SEM and TEM images of the SiO₂ nanospheres prepared by the *Stöber* method. The SEM and TEM images reveal that the SiO₂ nanospheres (ca. 240 nm in diameter) exhibit a uniform and relatively smooth spherical morphology over a wide scope.

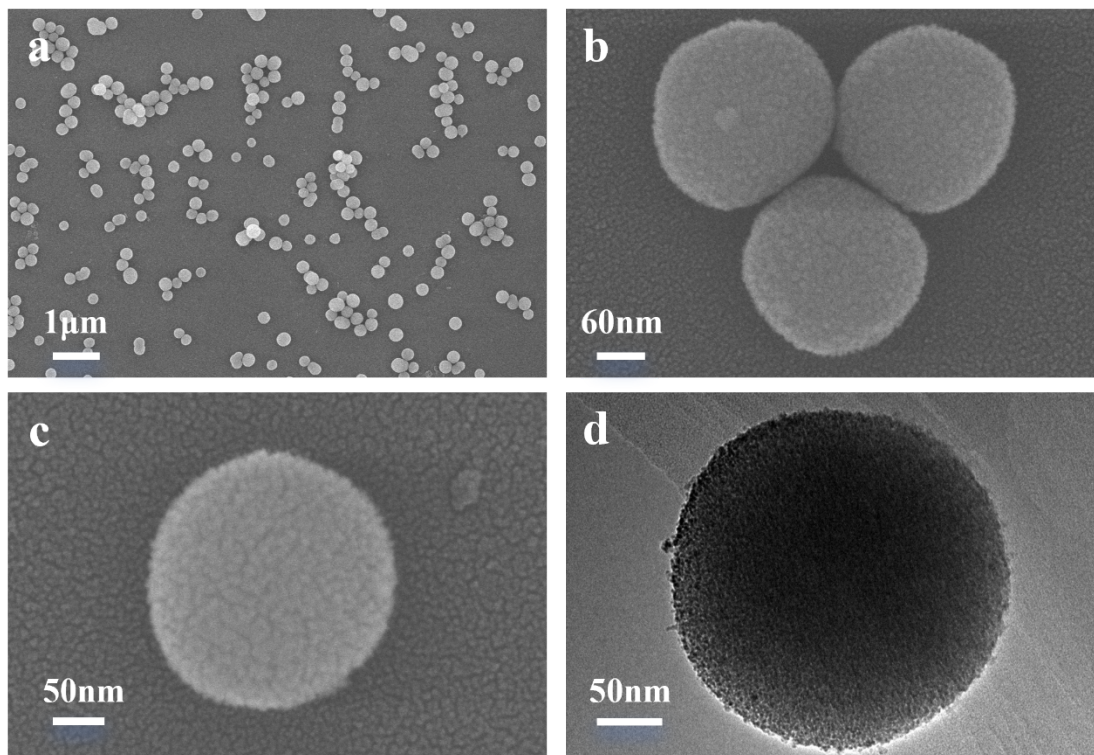


Figure S2. SEM and TEM images of the SiO₂@CeO₂ composite abrasives.

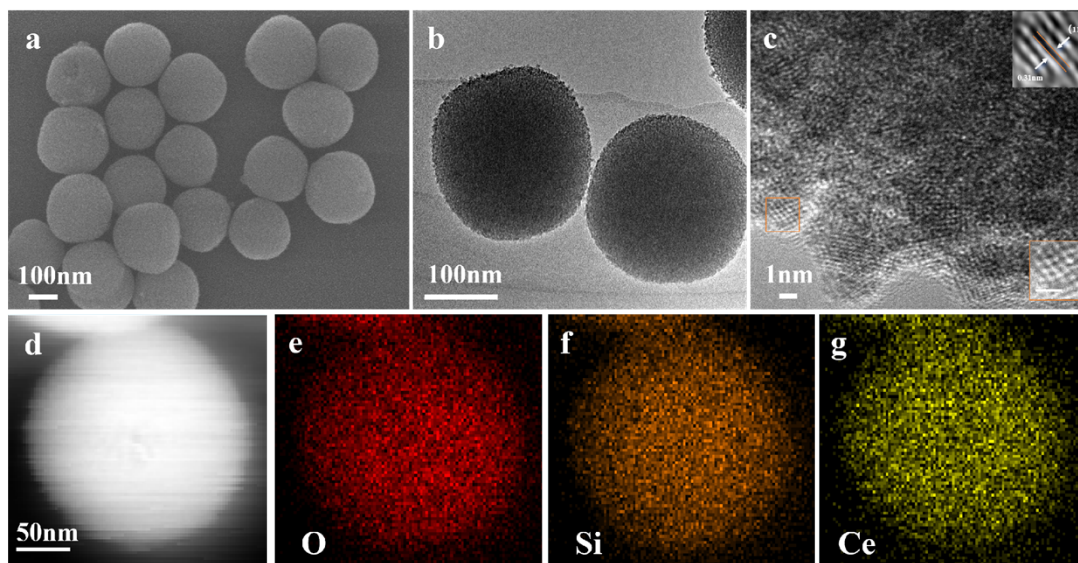


Figure S3. SEM (a), low- and high-resolution TEM (b, c) images of the SiO₂@CeO₂ composite abrasives, which show the anisotropic growth of the lattice orientation along the (111) crystal plane in different regions. High-angle annular darkfield scanning TEM (HAADF-STEM) image (d) and energy dispersive X-ray spectroscopy (EDS) elemental mapping images of O (e), Si (f), Ce (g) of SiO₂@CeO₂ composite abrasives.

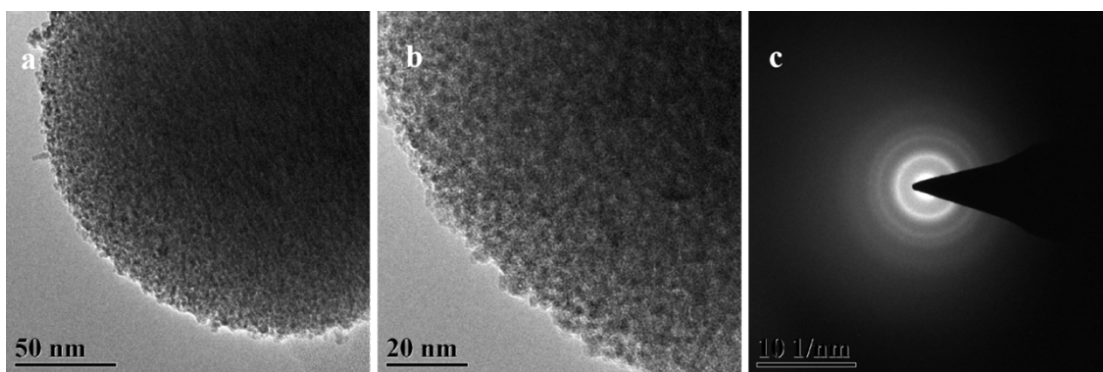


Figure S4. (a, b) HR-TEM images of the SiO₂@CeO₂ composite abrasives at different magnifications. (c) Lattice and selected electron diffraction patterns of the SiO₂@CeO₂ composite abrasives. No well-resolved diffraction rings can be observed in the high-resolution transmission electron microscopy (HRTEM) image and SAED pattern indicating the amorphous characteristics of such monodisperse SiO₂@CeO₂ composite abrasives.

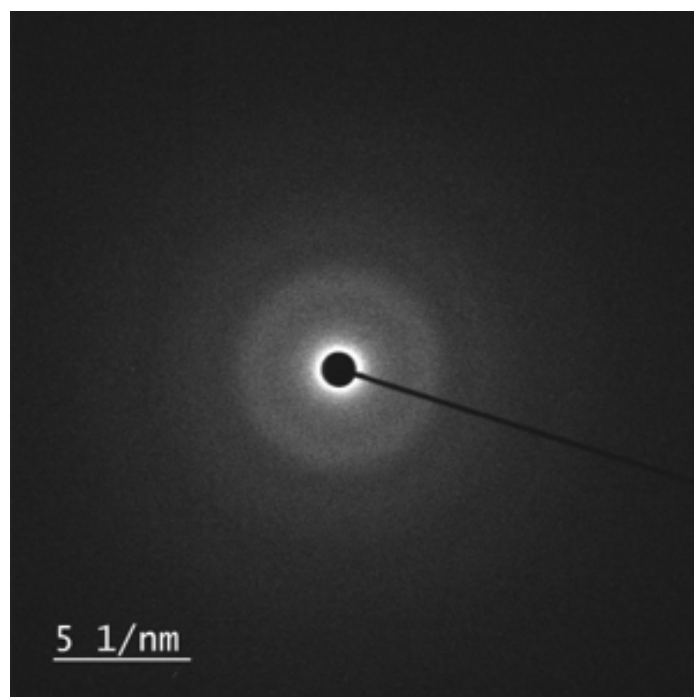


Figure S5. Selected area electronic diffraction (SAED) pattern, indicating the amorphous characteristics of such monodisperse $\text{SiO}_2@\text{CeO}_2@\text{PDA}$ composite abrasives.

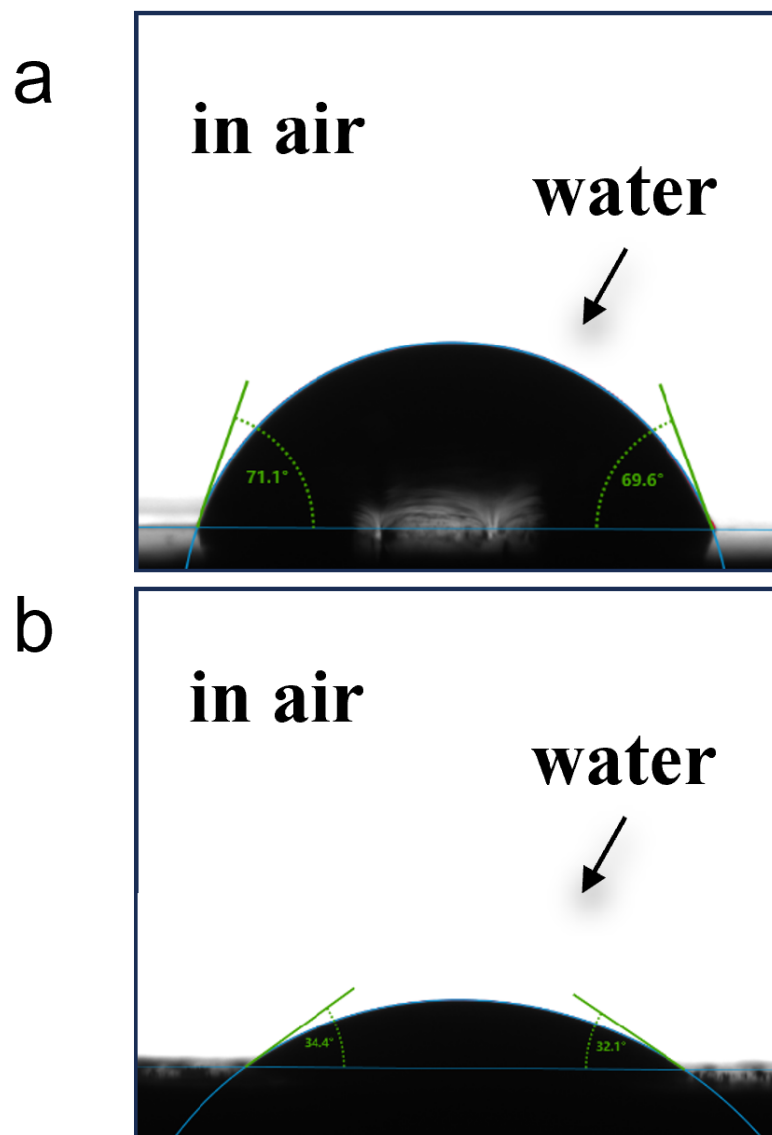


Figure S6. The contact angle (CA) of SiO₂@CeO₂ (a) and SiO₂@CeO₂@PDA (b) composite abrasives on the SiO₂ wafer. The results showed that the hydrophilicity of the dopamine-modified abrasives was significantly enhanced.

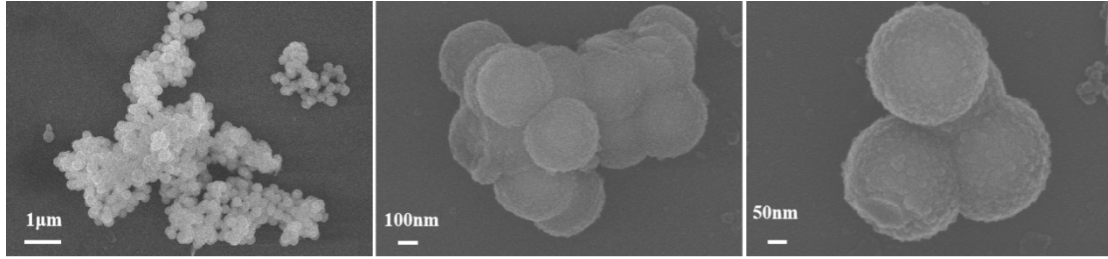


Figure S7. SEM(a), (b), (c) images of the SiO₂@CeO₂@PDA (16h) composite abrasives at different magnifications. While the reaction time was increased to 16 h, the further disordered growth of PDA resulted in serious abrasive agglomeration.